Estimation of Wood Density without Weighing Using Bending Vibration and Static Bending Tests – Effect of Span-to-Height Ratio on the Estimation Accuracy

Yoshitaka Kubojima,[a,]* Hideo Kato,[a] Satomi Sonoda,[b] and Kazuki Nanko [c]

The effects of the span-to-height ratio of wooden cantilevers on density estimation using bending vibration and static bending tests were examined. Bending vibration and static bending tests were performed for wooden cantilevers with various span-to-height ratios, and the densities of wooden cantilevers were estimated based on the measurements. The end condition of the cantilever was apart from the ideal condition for the smaller span-to-height ratios and approached to the ideal condition with the increase in the span-to-height ratio. The accuracy of the density without the correction decreased as the span-to-height ratio decreased. After correction based on the ideality of the end condition, the density could be accurately estimated without weighing the specimen.

DOI: 10.15376/biores.20.4.10521-10531

Keywords: Bending vibration; Cantilever; Density; Fixed end; Static bending

*Contact information: a: Department of Wood Properties, Forestry and Forest Products Research Institute, 1 Matsunosato, Tsukuba, Ibaraki, 305-8687 Japan; b: The Polytechnic University of Japan, 2-32-1 Ogawa-nishimachi, Kodaira-shi, 187-0035, Tokyo, Japan; c: Tokyo University of Agriculture and Technology, 3-5-8 Saiwaicho, Fuchu-shi, 183-8509, Tokyo, Japan; *Corresponding author: kubojima_yoshitaka580@ffpri.go.jp*

INTRODUCTION

Determining the density and Young's modulus of wood used for members such as columns and beams in constructions and beams for timber guardrails nondestructively is important. Determining the density and Young's modulus of the stored wood such as lumber in a stack, piled logs, piled round bars, and standing trees nondestructively is also important. They can be measured using static bending or bending vibration tests.

Although the Young's modulus of wood can be measured using the static bending test, the density cannot be measured with this method. The specific Young's modulus of wood can be calculated from the resonance frequency generated by the bending vibration test, but the density (mass) is required to calculate the Young's modulus. It is difficult to weigh the wood actually used for the members, the stored wood and the standing tree on site because removing each specimen from wood constructions, timber guardrails and stacks, or uprooting trees are time consuming.

A vibration testing method for wood using the reduction of resonance frequency due to mass addition (hereafter, referred to as the vibration method with additional mass, VAM) has been developed. The specimen mass and Young's modulus can be calculated without weighing using this method (Kubojima 2025).

VAM uses an appropriate mass ratio (attached mass to a specimen/specimen mass) (Sonoda *et al*. 2016), and a large attached mass is needed for large, or in other words, heavy piece of wood. Consequently, the work efficiency may be reduced in such a case. Changes in resonance frequencies caused by the additional mass of long specimens are small because the resonance frequencies are low. Thus, the accuracy of VAM may decrease for long specimens (Kubojima *et al*. 2024).

A method for estimating the density of wooden cantilevers using the Young's modulus obtained from the static bending test and the specific Young's modulus obtained from the bending vibration test (hereafter, referred to as the static and vibration hybrid method) (Kato *et al*. 2025) was developed to compensate for the inaccuracy of VAM for large specimens. Although there are studies using both vibration and static bending tests in combination that estimate the strength based on the positive relationship between the dynamic Young's modulus and strength (Aratake *et al*. 1992; Nakamura 1972; Nakayama 1968; 1975; Nakayama and Fujiwara 1977; Nakayama and Yoshiaki 1974), there has been a lack of studies estimating the density. The bending vibration of a specimen with a fixed condition is affected by the shear deflection, rotatory inertia, and semi-rigid of the end condition. These parameters depend on the span-to-height ratio of a specimen (Kubojima *et al*. 2006, 2012, 2022). Thus, the effect of the span-to-height ratio on the static and vibration hybrid method was investigated. Because this study is at an early stage, small clear rectangular specimens were used and the linear segment of the static bending load and deflection relationship was considered.

ESTIMATION OF WOOD DENSITY WITHOUT WEIGHING WOOD USING BENDING VIBRATION AND STATIC BENDING

The bending vibration and static bending under fixed-free conditions are considered in this work. For thin specimens with a constant cross-section, only pure bending needs to be accounted for.

The resonance frequency, denoted by f_n (n refers to the resonance mode number), can be expressed as follows,

$$f_n = \frac{1}{2\pi}\left(\frac{m_n}{l}\right)^2 \sqrt{\frac{EI}{\rho A}} \tag{1}$$

where E, I, l, ρ, and A are Young's modulus, the second moment of the area, the span, the density, and the cross-sectional area, respectively. The constant m_n depends on the vibration modes and can be expressed as follows.

$$m_1 = 1.875, m_2 = 4.694, m_3 = 7.855, m_n = \frac{1}{2}(2n-1)\pi \ (n > 3) \tag{2}$$

When the free end of a cantilever is loaded during the static bending, the slope of the linear segment of the static bending load (P) - deflection at the free end (y) diagram is expressed as follows.

$$\frac{dP}{dy} = 3\frac{EI}{l^3} \tag{3}$$

Based on Eqs. 1 and 3,

$$\rho = \frac{1}{3Al}\frac{dP}{dy}\left(\frac{m_n^2}{2\pi f_n}\right)^2 \text{ (Sonoda } et\ al.\text{ 2022)} \tag{4}$$

For the bending vibration of the actually used wood, the contributions of deflections due to shear and rotatory inertia to the total measured bending deflection cannot be negligible if the specimen is not thin (Timoshenko 1921). Additionally, the fixed end condition of the actually used wood is not the ideal fixed condition but rather a semi-rigid condition, which lies between the simply-supported condition and the fixed condition (Kubojima *et al*. 2022). Therefore, Eq. 1 is modified for the actually used wood as follows,

$$f_{n\mathrm{M}} = \frac{1}{2\pi}\left(\frac{m_{n\mathrm{M}}}{l}\right)^2 \sqrt{\frac{EI}{\rho A}} = \frac{1}{2\pi}\left(\frac{m_n}{l}\right)^2 \sqrt{\frac{E_{\mathrm{avib}} I}{\rho A}} \tag{5}$$

where subscripts M, a, and vib denote measured, apparent, and vibration, respectively.

From Eqs. 1 and 5, k_{vib} expressed by Eq. 6 can be obtained. The quantity k_{vib} is used as the index that indicates the degree of ideality of the end condition including the contributions of shear, rotatory inertia, and the semi-rigid condition in the bending vibration. When k_{vib} is equal to 1, the end condition is ideal.

$$k_{\mathrm{vib}} = \frac{f_{n\mathrm{M}}}{f_n} = \left(\frac{m_{n\mathrm{M}}}{m_n}\right)^2 = \sqrt{\frac{E_{\mathrm{avib}}}{E}} \text{ (Kubojima } et\ al. \text{ 2022)} \tag{6}$$

For the static bending of the actually used wood, the contribution of deflection due to shear to the total measured bending deflection cannot be negligible if the specimen is not thin (Timoshenko and Gere 1972). Additionally, the fixed end condition of the actually used wood is in the semi-rigid condition as mentioned above. Therefore, Eq. 3 is modified for the actually used wood as follows,

$$\left(\frac{dP}{dy}\right)_{\mathrm{M}} = 3\frac{E_{\mathrm{asb}} I}{l^3} \tag{7}$$

where the subscript sb denotes static bending.

Because the degree of ideality of the end condition in bending vibration is expressed by the square root of the Young's modulus ratio, as shown in Eq. 6, the square root of the Young's modulus ratio is expressed by Eq. 8 as the index that indicates the degree of ideality of the end condition including the contributions of shear and the semi-rigid condition in the static bending. When k_{sb} is equal to 1, the end condition is ideal.

$$k_{\mathrm{sb}} = \sqrt{\frac{E_{\mathrm{asb}}}{E}} \tag{8}$$

From Eqs. 5 and 6,

$$\frac{EI}{l^3} = \left(\frac{2\pi f_{n\mathrm{M}}}{m_{n\mathrm{M}}^2}\right)^2 \rho A l \tag{9}$$

From Eqs. 7 and 8,

$$\frac{EI}{l^3} = \frac{1}{3k_{\mathrm{sb}}^2}\left(\frac{dP}{dy}\right)_{\mathrm{M}} \tag{10}$$

From Eqs. 9 and 10,

$$\rho = \frac{1}{3Al}\left(\frac{k_{\mathrm{vib}}}{k_{\mathrm{sb}}}\right)^2 \left(\frac{dP}{dy}\right)_{\mathrm{M}} \left(\frac{m_n^2}{2\pi f_{n\mathrm{M}}}\right)^2 \tag{11}$$

The specimen mass can be estimated using the indices k_{vib} and k_{sb}, the slope of load-deflection diagram in static bending, and the resonance frequency in the bending vibration. The true Young's modulus E is measured under the ideal end condition, for example, a free-free longitudinal vibration test. The resonance frequency f_n is estimated by substituting E into Eq. 1, and k_{vib} is calculated by substituting f_n and the measured $f_{n\mathrm{M}}$ into Eq. 6. The apparent Young's modulus in the static bending E_{asb} is obtained by substituting $(dP/dy)_M$ into Eq. 7, and k_{sb} is calculated by substituting E and E_{asb} into Eq. 8. Thus, the density can be calculated by using Eq. 11. The specimen mass is not required for these calculations.

EXPERIMENTAL

Materials

Sitka spruce (*Picea sitchensis* Carr.) rectangular bars with a width of 25 mm (radial direction, R), heights of 5, 10, 15, 20, and 25 mm (tangential direction, T), and a length of 300 mm (longitudinal direction, L) were used as specimens. The specimens with no knots and with straight grain were cut from mainly heartwood. The specimens had an accurate longitudinal-radial, longitudinal-tangential, and radial-tangential planes. The surface of each specimen was finished with a tip saw. Three specimens for each dimension were used. The specimens were conditioned at 20 °C and 65% relative humidity until the weight became constant. All tests were conducted under the same conditions.

Free-free Longitudinal Vibration Test

To determine the true Young's modulus, the longitudinal vibration tests were conducted, and the resonance frequency of the first mode was measured. The free-free longitudinal vibration tests were conducted according to the following procedure (Kubojima *et al*. 2014). The specimen was placed at the nodal positions of the free-free longitudinal vibration corresponding to its first resonance mode. The longitudinal vibration was initiated by hitting the RT-plane of the specimen at one end using a wooden hammer (hammer head: 5 mm × 6 mm × 10 mm, 0.85 g), whereas the specimen motion was detected using a microphone (PRECISION SOUND LEVEL METER 2003, NODE Co., Ltd., Tokyo, Japan) at the other end. The direction of the microphone was parallel to the L-direction. The signal was processed using a fast Fourier transform (FFT) digital signal analyzer (Multi-Purpose FFT Analyzer CF-5220, Ono-Sokki, Co., Ltd., Yokohama, Japan) to obtain high-resolution resonance frequencies of the first resonance mode.

Bending Vibration Test for a Cantilever

The bending vibration tests for a cantilever were conducted according to the following procedure. An apparatus (Takachiho Seiki Co., Ltd., End condition controller KS-200) shown in Fig. 1 was used to provide different end conditions. The 25 mm (L) ×25 mm (R) region from an end was supported by the post of the apparatus whose cross section was 25 mm × 25 mm. Consequently, the span was 275 mm. The specimen was compressed by screwing a bolt attached to a load cell. It is thought that the vertical displacement was almost 0 and the rotation was partially restrained at the end. The compression stress was more than 2.6 MPa because the end condition was stable at the compression stress (Kubojima *et al*. 2022). The compression load was measured using the load cell and recorded using a data logger. Bending vibration was initiated by hitting the LR-plane of the specimen in the vertical direction at the tip using the aforementioned wooden hammer. The specimen motion was detected by the aforementioned microphone installed at the free end. The signal was processed using the aforementioned FFT digital signal analyzer to generate high-resolution resonance frequencies. Because the stress relaxation was observed for each set compressive stress, the vibration test was conducted when the load change became sufficiently small.

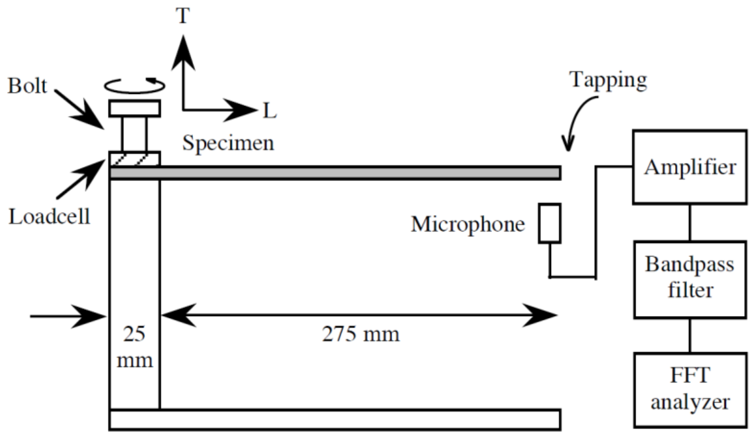

Fig. 1. Schematic diagram of the experimental setup for the bending vibration test under various end conditions

Free-free Bending Vibration Test

To obtain the shear modulus by bending, free-free bending vibration tests were conducted according to the following procedure (Kubojima *et al*. 1996). The specimen was suspended using two threads at the nodal positions of the free-free vibration corresponding to its resonance mode. The bending vibration was initiated by hitting the LR-plane of the specimen at one end using a wooden hammer, whereas the specimen motion was detected using the aforementioned microphone at the other end. The signal was processed using the aforementioned FFT digital signal analyzer as a means to obtain high-resolution resonance frequencies.

The vibration test was conducted, and the resonance frequencies in the 1^{st} to 5^{th} modes were measured. The Young's modulus and shear modulus of the LT-plane were calculated using the Goens-Hearmon regression method based on the Timoshenko theory of bending (TGH method) (Timoshenko 1921; Goens 1931; Hearmon 1958). The Young's modulus in the absence of the contributions of shear and rotatory inertia and shear modulus could be obtained using the TGH method for bending vibration.

Static Bending Test for a Cantilever

The static bending tests for the cantilever were conducted according to the following procedure. The apparatus (Takachiho Seiki Co., Ltd., End condition controller KS-200) shown in Fig. 2 was used to provide different end conditions. A 25 mm (L) × 25 mm (R) region from an end was supported by the posts of the apparatus whose cross section was 25 mm × 25 mm. Consequently, the span was 275 mm. The specimen was compressed by screwing a bolt attached to the load cell. It is thought that the vertical displacement was almost 0 and the rotation was partially restrained at the end. The compression stress was more than 2.6 MPa because the end condition was stable at the compression stress (Kubojima *et al*. 2022). The compression loads at both ends were measured by the load cell and recorded using the data logger. The free end of the cantilever was loaded, and the load and deflection were measured using the apparatus (Takachiho Seiki Co., Ltd., K200O), as shown in Fig. 2. The cross-head speed was 5 mm/min.

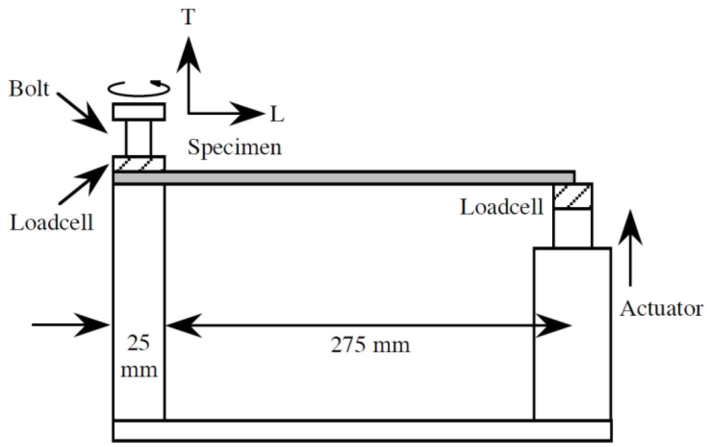

Fig. 2. Schematic diagram of the experimental setup for the static bending test under various end conditions

RESULTS AND DISCUSSION

The average (standard deviation) of the density, the Young's modulus measured using the longitudinal vibration test, and the shear modulus measured using the bending vibration test were 430 (26) kg/m^3, 12.36 (0.99) GPa, and 0.78 (0.11) GPa, respectively.

The examples of the relationships between the load and deflection of the static bending test are shown in Fig. 3.

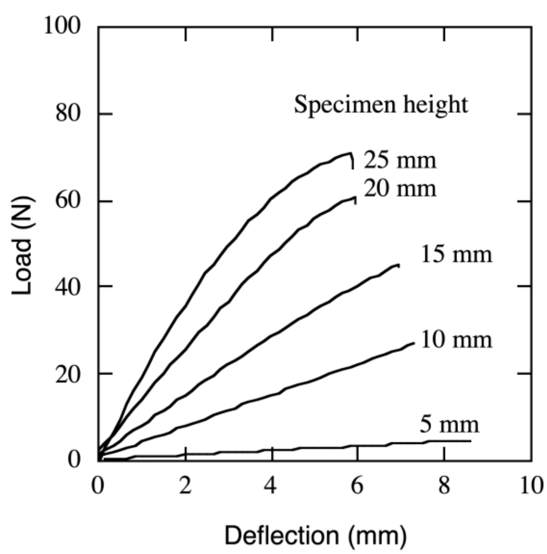

Fig. 3. Examples of the relationship between load and deflection during the static bending

Figure 4 shows the degree of ideality of the end condition for various span-to-height ratios. All the results were less than 1. The contributions of the shear and rotatory inertia are compared to that of the semi-rigid condition.

The frequency equation is expressed by Eq. 12, incorporating the contributions of deflections due to shear and rotatory inertia to the total measured bending deflection under the ideal fixed - free condition based on the Timoshenko theory of bending (Timoshenko 1921; Komatsu and Toda 1977; Akiyama *et al*. 2007).

$$2 + \left(\frac{\varepsilon}{\eta} + \frac{\eta}{\varepsilon}\right)\cos\beta m_{nt}\cosh\alpha m_{nt} + \left(\frac{\alpha}{\beta} - \frac{\beta}{\alpha}\right)\sin\beta m_{nt}\sinh\alpha m_{nt} = 0 \tag{12}$$

$$\alpha = \sqrt{\sqrt{B_{\mathrm{t}}^2 m_{nt}^4 + 1} - A_{\mathrm{t}} m_{nt}^2} \tag{13}$$

$$\beta = \sqrt{\sqrt{B_{\mathrm{t}}^2 m_{nt}^4 + 1} + A_{\mathrm{t}} m_{nt}^2} \tag{14}$$

$$\varepsilon = \sqrt{B_{\mathrm{t}}^2 m_{nt}^4 + 1} + B_{\mathrm{t}} m_{nt}^2 \tag{15}$$

$$\eta = \sqrt{B_{\mathrm{t}}^2 m_{nt}^4 + 1} - B_{\mathrm{t}} m_{nt}^2 \tag{16}$$

$$A_{\mathrm{t}} = \frac{I}{2Al^2}\left(\frac{sE_{\mathrm{t}}}{G} + 1\right) \tag{17}$$

$$B_{\mathrm{t}} = \frac{I}{2Al^2}\left(\frac{sE_{\mathrm{t}}}{G} - 1\right) \tag{18}$$

where s is the form factor (= 1.2 for a rectangular cross-section, Timoshenko and Gere 1972) and E_{t} is the Young's modulus based on the Timoshenko theory of bending, respectively.

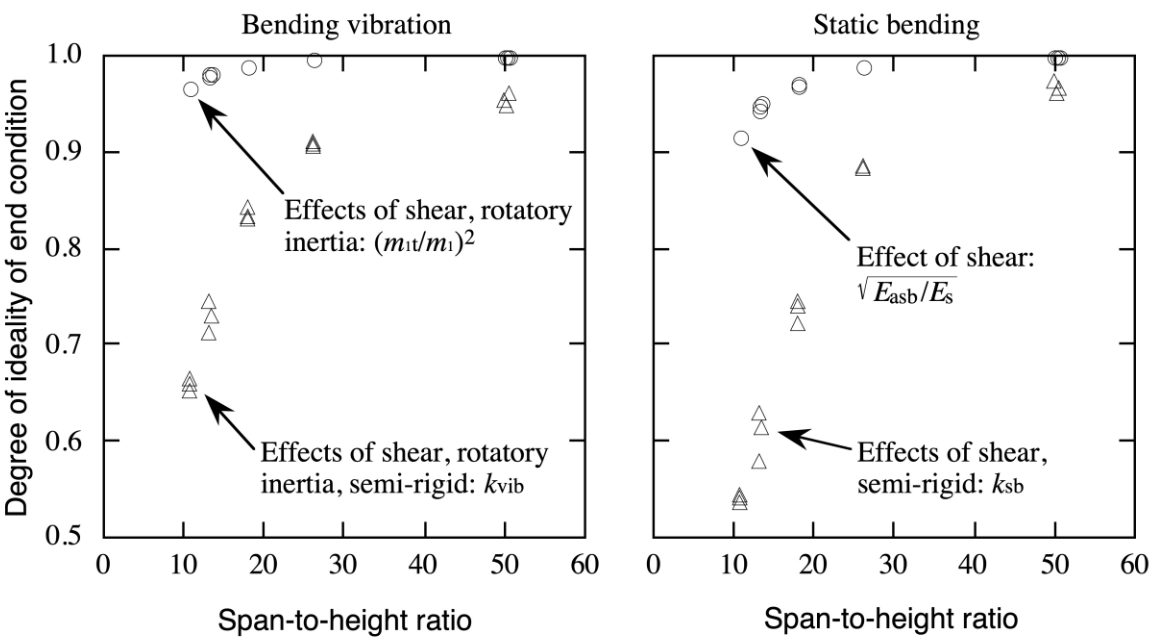

Fig. 4. The contributions of shear, rotatory inertia, and the semi-rigid condition at different the span-to-height ratios

Substituting the Young's modulus measured by the longitudinal vibration test into E_{t} in Eqs. 17 and 18, the shear modulus measured by the free-free bending vibration test into G in Eqs. 17 and 18 and the span-to-height ratio into Eqs. 17 and 18, m_{nt} can be obtained from Eq. 12. Mathematica 14.1J software (Wolfram Research Co., Ltd.) was used in the calculation. The ratio of $(m_{1t}/m_1)^2$ (m_1 = 1.875 in Eq. 2) was used as the index that indicates the degree of ideality of the end condition including the contributions of shear and rotatory inertia in the bending vibration. The value of $(m_{1t}/m_1)^2$ was apart from 1 for the smaller span-to-height ratios and approached to 1 with the increase in the span-to-height ratio, as shown in Fig. 4 (circles).

The static bending deflection of the rectangular specimen at x (x: distance along the specimen from the fixed end) under the ideal fixed - free conditions that is loaded at the free end taking into account the shear is expressed as follows (Timoshenko and Gere 1972),

$$\frac{Pl^3}{6E_sI}\left(\frac{x}{l}\right)^3\left(3-\frac{x}{l}\right)+\frac{sP}{GA}x=\frac{Pl^3}{6E_{\mathrm{asb}}I}\left(\frac{x}{l}\right)^3\left(3-\frac{x}{l}\right) \tag{19}$$

where the subscript s denotes the value without the contribution of shear.

When $x = l$ is substituted into Eq. 19,

$$\frac{E_\mathrm{s}}{E_\mathrm{asb}}=1+\frac{sE_\mathrm{s}}{4G}\left(\frac{h}{l}\right)^2 \tag{20}$$

The term $\sqrt{E_\mathrm{asb}/E_\mathrm{s}}$ was used as the degree of ideality of the end condition including the contribution of shear in the static bending. The value of $\sqrt{E_\mathrm{asb}/E_\mathrm{s}}$ is calculated by substituting the Young's modulus from the longitudinal vibration test into E_s in Eq. 20 and the shear modulus from the free - free bending vibration test into G in Eq. 20. The value of $\sqrt{E_\mathrm{asb}/E_\mathrm{s}}$ was apart from 1 for the smaller span-to-height ratios and approached to 1 with the increase in the span-to-height ratio, as shown in Fig. 4 (circles).

As shown in Fig. 4 (triangles), the values of $k_\mathrm{vib}=\frac{f_{n\mathrm{M}}}{f_n}$ from Eq. 6 and $k_\mathrm{sb}=\sqrt{E_\mathrm{asb}/E_\mathrm{s}}$ from Eq. 8 (E is from the free-free longitudinal vibration test) were apart from 1 for the smaller span-to-height ratios and approached to 1 with the increase in the span-to-height ratio. They decreased rather than $(m_{1\mathrm{t}}/m_1)^2$ from Eq. 12 and $\sqrt{E_\mathrm{asb}/E_\mathrm{s}}$ from Eq. 20. Thus, the effect of the semi-rigid condition was not negligible, especially for the smaller span-to-height ratios.

The estimated density using the static and vibration hybrid method was compared to the measured density in Fig. 5.

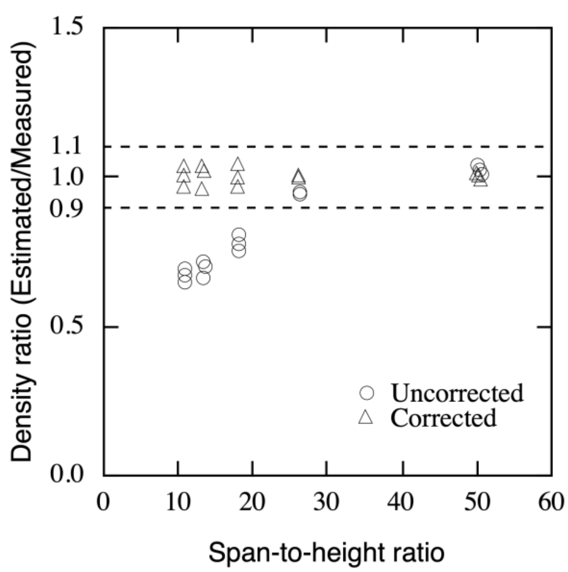

Fig. 5. Changes in the accuracy of the estimated density using the static and vibration hybrid method

When the density was calculated without correcting the ideality of the end condition, Eq. 4 was used and the measured slope $(dP/dy)_M$ and the measured resonance frequency f_{nM} were substituted into Eq. 4. The accuracy of the density without the correction decreased as the span-to-height ratio decreased. Thus, the density of specimens with smaller span-to-height ratios cannot be accurately calculated using Eq. 4.

A correction was formulated based on the ideality of the end condition. The means of k_{sb} and k_{vib} of the 3 specimens at each span-to-height ratio were substituted into Eq. 11. The resulting density was estimated at an accuracy of ±10%. Therefore, correction based on the ideality of the end condition improved the accuracy of the density estimates without weighing the specimen. If the variations of k_{sb} and k_{vib} are small within one site, for example, the site where timber piles are buried and the site where trees are planted, the extensive experimentation to obtain k_{sb} and k_{vib} are not necessary at the site.

Expected errors in this method due to non-ideal situations of simplifications are related to some simplifying assumptions that have been applied. The effect of air viscosity is assumed to be small because the change in the resonance frequency was only 0.3 to 1.1 % in the region of 760 to 1 mmHg (Kataoka and Ono 1975). When the results of this study are applied to actual wood such as flat square lumber, dimension lumber, beams of wood guardrails, and timber piles, Eq. (11) can be used because their cross sections are unform. Although the wood properties in the T-direction are considered to be uniform, those in the R-direction are not. The effect of the different layers in wood is small because the same second moment of the area is used for both bending vibration and static bending tests.

CONCLUSIONS

1. The end condition of cantilever showed an important difference from the ideal condition for the smaller span-to-height ratios and approached to the ideal condition with the increase in the span-to-height ratio.
2. The accuracy of the density without the correction decreased as the span-to-height ratio decreased.
3. After correction based on the ideality of the end condition, the density could be accurately estimated without weighing the specimen.

ACKNOWLEDGMENTS

This work was supported by JSPS KAKENHI Grant Number JP25K09230. This study was presented in part at the 42nd Annual Meeting of the Wood Technological Association of Japan, Kyoto, September 2024.

REFERENCES CITED

Akiyama, K., Kishino, Y, and Murai, S. (2007). "Discussion of applicability of the Timoshenko beam theory based on the exact theory of wave propagation," *Journal of Japan Society of Civil Engineers Series A* 63(1), 232-241.

Aratake, S., Arima, T., Sakoda, T., and Nakamura, Y. (1992). "Estimation of modulus of rupture (MOR) of lumber using higher natural frequency of log in pile of logs. Possibility of application for Sugi scaffolding board," *Mokuzai Gakkaishi* 38(11), 995-1001.

Goens, E. (1931). "Über die Bestimmung des Elastizitätsmodulus von Stäben mit Hilfe von Biegungsschwingungen," *Annalen der Physik 5F* 11, 649-678.

Hearmon, R. F. S. (1958). "The influence of shear and rotatory inertia on the free flexural vibration of wooden beams," *British Journal of Applied Physics* 9, 381-388.

Kataoka, A., and Ono, T. (1975). "The relations of experimental factors to the vibration and the measuring values of dynamic mechanical properties of wood I. The experimental errors due to the measuring apparatus," *Mokuzai Gakkaishi* 21(10), 543-550.

Kato, H., Kubojima, Y., Sonoda, S., and Beniya, N. (2025). "Evaluation of Young's modulus of wood using static and vibration hybrid methods," *Abstracts of the 75th Annual Meeting of the Japan Wood Research Society*, D20-02-1100.

Komatsu, K., and Toda, S. (1977). "Beam-type vibrations of short thin cylindrical shells," *Technical Report National Aerospace Laboratory* 502, 1-11.

Kubojima, Y. (2025). "Effect of mass addition on vibrational properties of wood and its application," *Journal of Wood Science* 71, article 42. DOI: 10.1186/s10086-025-02210-3

Kubojima, Y., Kato, H., and Tonosaki, M. (2012). "Fixed-fixed flexural vibration testing method of actual-size bars for timber guardrails," *Journal of Wood Science* 58(3), 211-215. DOI: 10.1007_s10086-011-1248-0

Kubojima, Y., Ohsaki, H., Kato, H., and Tonosaki, M. (2006). "Fixed-fixed flexural vibration testing method of beams for timber guardrails," *Journal of Wood Science* 52(3), 202-207. DOI: 10.1007/s10086-005-0754-3

Kubojima, Y., Sonoda, S., and Kato, H. (2022). "Application of a bending vibration method without weighing specimens to the practical wooden members conditions," *Journal of Wood Science* 68, article 39. DOI: 10.1186/s10086-020-01929-5

Kubojima, Y., Sonoda, S., and Kato, H. (2024). "Estimation of mass and moisture content of flat square lumber in a stack during air-drying process by the vibration method with additional mass," *Journal of Wood Science* 70, article 45. DOI: 10.1186/s10086-024-02158-w

Kubojima, Y., Suzuki, Y., and Tonosaki, M. (2014). "Effect of additional mass on the apparent Young's modulus of a wooden bar by longitudinal vibration," *BioResources* 9(3), 5088-5098. DOI: 10.15376/biores.9.3.5088-5098

Kubojima. Y., Yoshihara, H., Ohta, M., and Okano, T. (1996). "Examination of the method of measuring the shear modulus of wood based on the Timoshenko theory of bending," *Mokuzai Gakkaishi* 42(12), 1170-1176.

Nakamura, Y. (1972). "Studies on stress grading for structural laminae taken from woods in southern Kyushu," *Bulletin of the Miyazaki University Forests* 6, 1-82.

Nakayama, Y. (1968). "Studies on the dynamic Young's modulus of wooden beam (I) the dynamic Young's modulus and the bending strength," *Bulletin of the Kochi University Forest* 2, 17-32.

Nakayama, Y. (1975). "Non-destructive test of wooden beam by vibrational method. Estimation of modulus of rupture in bending of beam containing an artificial circular hole," *Mokuzai Gakkaishi* 21(7), 402-409.

Nakayama, Y., and Fujiwara, S. (1977). "Estimation of modulus of rupture in bending of wooden beam containing a square hole by vibrational method," *Research Reports of the Kochi University Agricultural Science* 26(15),143-154.

Nakayama, Y., and Yoshikai, Y. (1974). "Estimation of modulus of rupture in bending of sugi beam with knots by vibrational method," *Research Reports of the Kochi University Agricultural Science* 23(16), 155-166.

Sonoda, S., Kubojima, Y., and Kato, H. (2016). "Practical techniques for the vibration method with additional mass Part 2: Experimental study on the additional mass in longitudinal vibration test for timber measurement," *Proceedings of the World Conference on Timber Engineering*.

Sonoda, S., Kubojima, Y., Kato, H., and Hara, T. (2022). "Vibration and its application of wooden pile in the ground. Part 5. Static bending test," *Abstracts of the 72^th^ Annual Meeting of the Japan Wood Research Society*, Y16-06-1400.

Timoshenko, S. P. (1921). "On the correction for shear of the differential equation for transverse vibrations of prismatic bars," *Philosophical Magazine 6 Series* 41, 744-746.

Timoshenko, S. P., and Gere. J. M. (1972). *Mechanics of Materials*, D. Van Nostrand Company, New York, pp. 368-374.

Article submitted: July 25, 2025; Peer review completed: August 24, 2025; Revised version received: September 1, 2025; Accepted: October 4, 2025; Published: October 21, 2025.
DOI: 10.15376/biores.20.4.10521-10531